Open Access

Advances in Environmental and Engineering Research

LIDSEN Publishing Inc.

Research Article

Impact of COVID-19 Lockdowns and Australian Bushfires on Aerosol Loading over the Downwind Oceanic Regions

Xuepeng Zhao *

Oceanographic and Geophysical Science and Services Division (OGSSD) , National Centres for Environmental Information (NCEI), NOAA/NESDIS, 1315 East-West Hwy, SSMC3, RM-4661, Silver Spring, MD 20910-3282, USA; E-Mail: xuepeng.zhao@noaa.gov

* **Correspondence:** Xuepeng Zhao; E-Mail: xuepeng.zhao@noaa.gov

Academic Editor: Alfredo Moreira Caseiro Rocha

Special Issue: Remote Sensing on Climate Change

Adv Environ Eng Res
2020, volume 1, issue 4
doi:10.21926/aeer.2004003

Received: August 21, 2020
Accepted: November 17, 2020
Published: November 23, 2020

Abstract

Nearly 40 years of aerosol optical thickness (AOT) climate data record (CDR) from AVHRR satellite observations over the global ocean is used to study the impact of COVID-19 lockdowns and Australian bushfires on aerosol loading over downwind oceanic regions. Recent similar impact studies, by contrast, were mainly focused on the urban and suburban areas near the emission sources. AOT is used as a proxy for aerosol loading in our study. We found that AOT variations due to anthropogenic emission reduction during the lockdown period are complex and non-linear. AOT reduction was observed over China's east coastal oceans due to emissions reduction during the stringent lockdown period in China. However, an unexpected surge of AOT occurred over the coastal oceans of India during the tight lockdown period in the pre-monsoon season. Moreover, inter-annual variations of AOT, along with a long-term decreasing trend, may conceal the lockdown-related AOT changes over the US east coastal ocean and the Mediterranean Sea due to relatively relaxed lockdown measures. By contrast, AOT increases in a monotonic way due to the emissions from severe Australian bushfires in the 2019/2020 fire season. The AOT surge is evident not only over the Australian coastal ocean but also extends to the entire southern ocean. This comparative

study of two opposite extreme emission scenarios in natural conditions could be a benefit in creating effective mitigation strategies for future anthropogenic emissions and air pollution.

Keywords
Satellite observation; climate data record (CDR); aerosol optical thickness (AOT); Australia; anthropogenic emission; coronavirus disease 2019 (COVID-19); bushfire

1. Introduction

The coronavirus disease 2019 (COVID-19) pandemic resulted in a disaster for global public health and human life [1]. In order to effectively contain the spread of the coronavirus, confinement polices of varying stringency and extent have been implemented in affected countries and regions. Unintentionally, pollution emissions associated with anthropogenic activities were reduced during the period of lockdown [2-4]. As a result, air quality was also altered unexpectedly, especially in countries or regions plagued by both heavy anthropogenic pollution and COVID-19 [2, 5-10]. Recent studies on the impact of COVID-19 lockdowns on air quality are mainly focused in the urban and suburban areas near emission sources. For example, Le et al. (2020) [11] studied the aerosol loading changes in northern China during the initial lockdown period. Their study indicated that extreme particulate matter levels unexpectedly occurred in northern China due to favourable meteorological conditions for heterogeneous chemistry, non-linear gas-phase chemistry, and titration of ozone in winter. Wang et al. (2020) [12] further found that some severe air pollution events may not be avoided by reduced anthropogenic activities during COVID-19 lockdowns in China when meteorological conditions are unfavourable.

On the other hand, Australian bushfires occurred at nearly the same time as the initial COVID-19 outbreak in China, severely damaging the air quality of Australia[13, 14]. The smoke plumes reached the entire southern ocean as well as the lower stratosphere [15, 16]. The severe bushfires and associated emissions created serious environmental and health consequences [17, 18]. These two opposite extreme cases of surface emissions related to human and natural disasters provide us a unique opportunity for a comparative study of the impact of surface emissions on air pollution in natural conditions, which will benefit mitigation strategies for air pollution emissions. In this paper, we use the long-term satellite climate data record (CDR) of aerosol optical thickness (AOT) as a proxy for aerosol loading to study the impact of COVID-19 lockdowns and Australian bushfires on AOT in the downwind oceanic regions influenced by offshore airflows originating from the lockdown continents and Australian burning grounds. Long-term satellite AOT CDR is introduced in section 2; the analysis approach is described in section 3; the impact of COVID-19 lockdowns and Australian bushfires on downwind aerosol loading in five selected coastal oceanic regions is investigated in section 4; summary and conclusions are given in the closing section.

2. Data

Version 3 of the Advanced Very High Resolution Radiometer (AVHRR) aerosol optical thickness CDR [19, 20] from National Oceanic and Atmospheric Administration (NOAA) operational satellites

is used in this study. AVHRR AOT CDR is derived over the global ocean surface for 0.63μm channel from AVHRR clear-sky daytime reflectance based on a two-channel retrieval algorithm [21]. A weak absorption aerosol model with a bimodal lognormal size distribution is used in the algorithm to account for accumulation and coarse modes. Please refer to Zhao et al. (2004) [21] for more information on the retrieval algorithm and performance. The AVHRR AOT CDR product had been used to study AOT long-term trends and aerosol cloud interactions [19, 20, 22, 23]. AOT CDR spans from 1981 to present and operationally forward updated on a quarterly basis. Both daily and monthly products in a spatial resolution of 0.1° x 0.1° degree are available (http://doi.org/10.7289/V5BZ642P), but only the latter is used in the current study. We also use the reanalysis surface wind speed at 10m and 850mb altitude in our analysis to examine the possible airflow transport effect. The wind speed data is obtained from the National Centers for Environmental Prediction (NCEP) climate forecast system reanalysis (CFSR) [24] monthly mean product (ftp://nomads.ncdc.noaa.gov/CFSR/HP_monthly_means/).

Five downwind oceanic regions that are often influenced by offshore pollutants from the continents, and that were also under the influence of COVID-19 lockdowns or Australian bushfires, are selected in our study and listed in Table 1. The latitude and longitude coverage and the months in which we are interested are also provided in the table. Two big cities located on the coastal line of each of the five coastal regions are also selected for our study. A square area of ±5° latitude and longitude around the big cities is used in our analysis.

Table 1 Five oceanic regions along with two associated coastal cities and the months selected for study.

Region Number	Regions and Cities	Longitude, Latitude	Month	Notes
1	East oceans of China	115°E − 135°E, 20°N − 40°N	January-June 2020	Influenced by lockdown
	Shanghai	31.2304°N ± 5°, 121.4737°E ± 5°		
	Tianjin	39.3434°N ± 5°, 117.3616°E ± 5°		
2	Mediterranean Sea	-15°W − 30°E, 30°N − 45°N	March−June 2020	Influenced by lockdown
	Barcelona	41.3851oN ± 5°, 2.1734°E ± 5°		
	Rome	41.9028°N ± 5°, 12.4964°E ± 5°		
3	East ocean of USA	-80°W − -70°W, 30°N − 45°N	March−June 2020	Influenced by lockdown
	New York City	40.7128°N ± 5°, -74.006°W ± 5°		
	Charleston	32.7765°N ± 5°, -79.9311°W ± 5°		
4	Coastal oceans of India	65°E − 90°E, 10°N − 25°N	March−June 2020	Influenced by lockdown
	Mumbai	19.0760°N ± 5°, 72.8777°E ± 5°		
	Chennai	13.0821°N ± 5°, 80.2707°E ± 5°		
5	East coastal ocean of Australia	140°E − 155°E, -40°S − -20°S	November 2019 −February 2020	Influenced by bushfires
	Melbourne	-37.8136°S ± 5°, 144.9631°E ± 5°		
	Sydney	-33.8688°S ± 5°, 151.2093°E ± 5°		

3. Approach

Offshore airflows may travel hundreds to thousands of kilometres from the emission source regions over land to downwind oceanic areas, where AOT changes are not necessary linearly correlated with the emission changes in source regions. This is due to the complex chemical and microphysical changes of aerosol particles during the transport, along with the effects of meteorological conditions. Thus, two types of monthly AOT difference are computed for the five selected regions and two associated big cities to assess the impact of lockdowns (or bushfires) on the aerosol loading in our study. The first type is the monthly AOT difference between selected months of 2019/2020 with the influence of the COVID-19 pandemic (or Australian bushfires) and the corresponding months of 2018/2019 without these influences. Similar difference analyses were widely used recently in assessing the lockdown's impact on air quality near urban emission source regions.

The second type of AOT difference is the monthly AOT anomaly for selected months of 2019/2020 with the influence of the COVID-19 pandemic (or Australian bushfires) relative to their corresponding monthly climatology, which is barely used in the other impact studies of COVID-19 lockdowns even though anomaly computation had been widely used for detecting other atmospheric phenomena. Thirty-five years of monthly AOT CDR, from January 1981 to December 2015, are used to compute AOT climatology for individual months. For example, the AOT climatology value of January at a spatial grid point is the arithmetical mean of 35 January values from 1981 to 2015. Even though emission changes due to the lockdown may be one of the major causes of AOT variations near the emission sources, this is not necessary the case for downwind coastal oceans, where AOT variation due to the lockdown is relatively weak in comparison to the urban areas near emission sources. Thus, other AOT variations, such as the inter-annual variation (including long-term trends), may conceal the AOT change due to the lockdown and make it indiscernible in satellite observations over the coastal oceans.

Consistent results obtained from the above two types of monthly AOT differences for the cases with and without lockdowns (or bushfires) should be more useful in assessing the impact of lockdowns (or bushfires) than the results based solely on either one of them. Figure 1 shows examples of the two types of monthly AOT differences over the global oceans for January and February 2020. The two types of AOT differences are presented in a relative percentage. It is seen that the two types of AOT differences show consistent AOT enhancement (> 90%) over the entire southern ocean due to the strong emissions from severe Australia bushfires in both January and February 2020. Even though inconsistencies exist evidently and broadly in the two types of AOT differences over the northern oceans, consistent AOT reduction in both AOT differences are also evident in some specific regions, such as over the Mediterranean Sea and the Chinese Yellow Sea. Since the COVID-19 lockdown started in later January 2020 in China, it is interesting to study whether the emissions reduction due to the lockdown contributes to the AOT reduction noticed in the downwind east oceanic regions of China. Therefore, we selected five offshore downwind oceanic regions along with two big coastal cities in each of the five regions (see Table 1) to examine the signature of COVID-19 lockdowns or the Australian bushfires contained in the change of AOT.

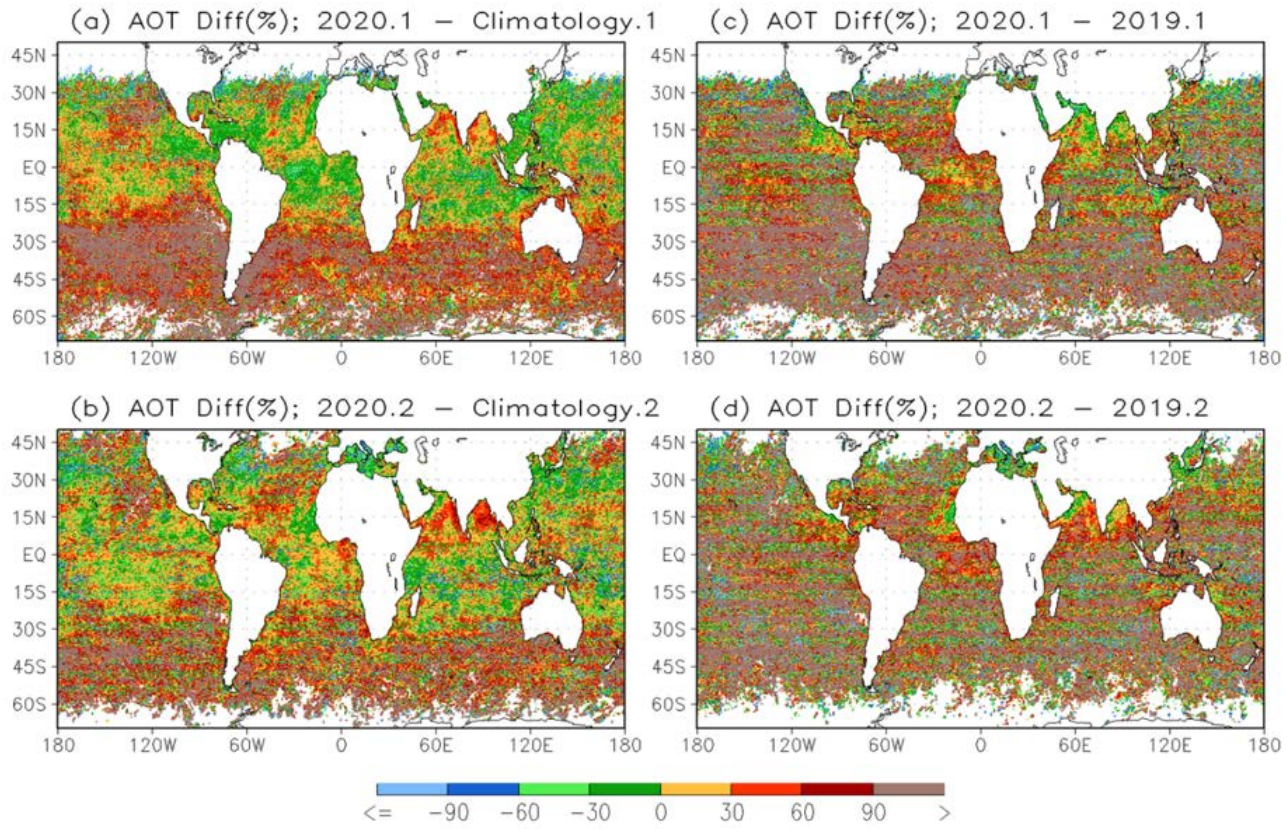

Figure 1 Distributions of relative monthly AOT anomaly (in percentage) over the global oceans for the lockdown/bushfire months of (a) January and (b) February 2020 and the distributions of relative monthly AOT difference (in percentage) between the lockdown/bushfire months of (c) January and (d) February 2020 and the corresponding months without lockdown/bushfire in 2019.

4. Results

4.1 AOT and COVID-19 Lockdown

The outbreak of COVID-19 pandemic in Wuhan occurred in December 2019 and the lockdown started being implemented in late January 2020 in China in order to prevent the spread of the coronavirus. The lockdown was gradually lifted from March to June 2020 based on the status of the coronavirus in individual provinces. Air quality was improved unintentionally in urban areas of China due to the reduction of gas and particle pollutants (e.g., CO, NO_2, SO_2, $PM_{2.5}$, and PM_{10}) from anthropogenic activities during the lockdown period [25, 26]. Figure 2 shows the relative difference of monthly AOT during the lockdown period of 2020 from their corresponding monthly climatology and the corresponding monthly AOT of 2019 over the east oceans of China. Capital letters S(hanghai) and T(ianjin) in Figure 2a mark the positions of the two selected coastal cities. The dashed or solid contour lines mark the areas where negative or positive AOT difference is above the 5% significance level, which is defined as when the negative or positive difference is larger than two times the standard deviation. The standard deviation of AOT difference for a grid point is calculated from the AOT difference at surrounding 5 x 5 grid points. Both types of monthly AOT difference show that AOT can be reduced up to 60% or with a reduction significance above the 5% level in January and

February over the east oceans of China. In March, the two types of monthly AOT differences show consistent reductions only in the central part of the east oceans since the lockdown was somewhat eased and industrial production was partially restored in China. Inconsistence in the two types of monthly AOT differences over the east oceans appears in April, May, and June when the lockdown was lifted gradually, which suggests that meteorological conditions may have changed and associated AOT inter-annual variabilities probably become dominant, thereby concealing the AOT changes induced by the confinement measures when the lockdown was eased.

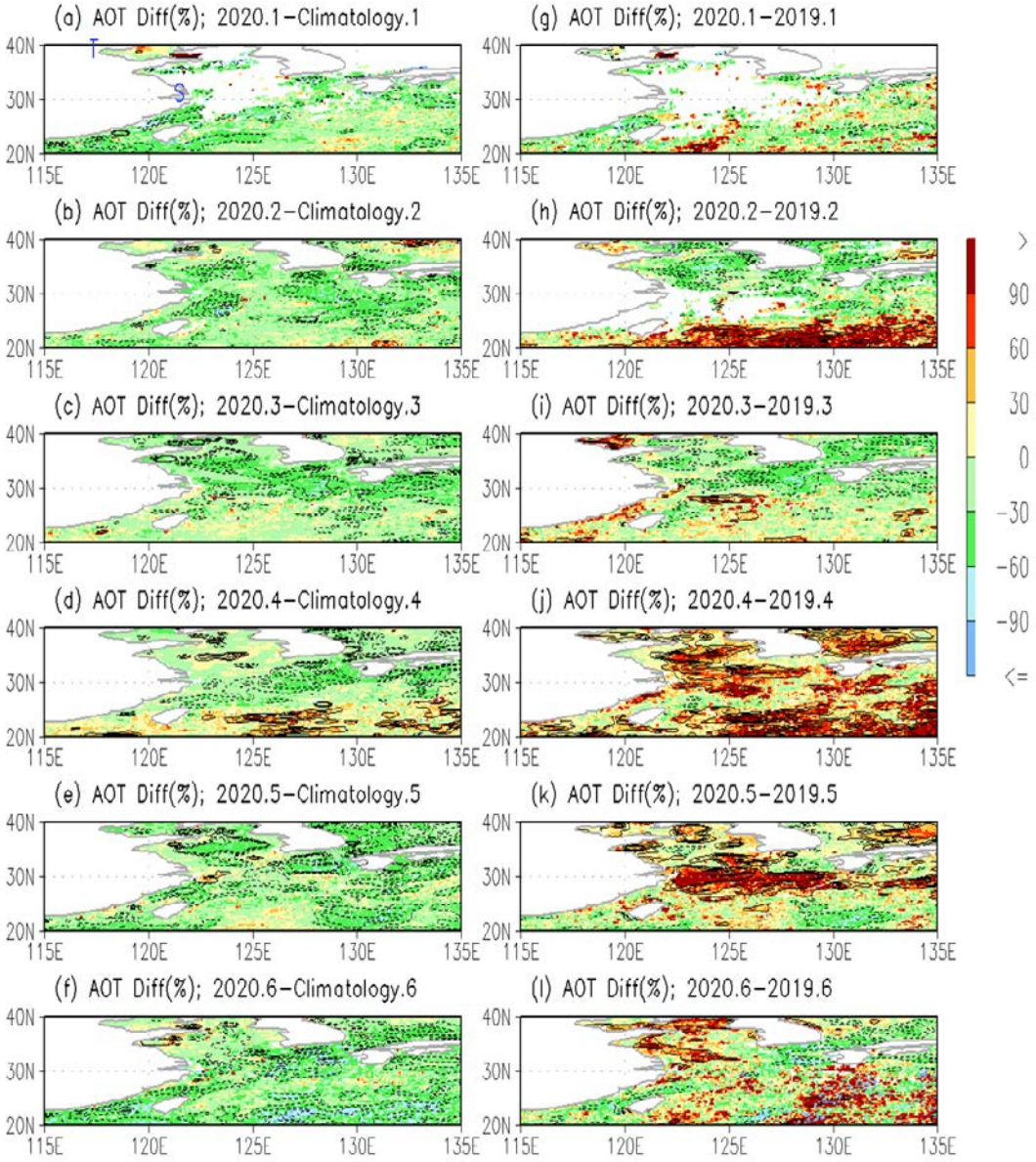

Figure 2 Distributions of relative monthly AOT anomaly (%) over the east oceanic regions of China (left panels) for the lockdown months of 2020 along with the distributions of relative monthly AOT difference (%) between lockdown months in 2020 and the corresponding months without lockdown in 2019 (right panels). Blue capital letters S(hanghai) and T(ianjin) in panel (a) mark the positions of the two selected coastal cities. The dash and solid contour lines mark the areas where the AOT difference is above negative and positive 5% significance level, respectively.

To support our interpretation, we further plot out AOT distribution overlaid with CFSR reanalysis surface wind speed at 10m altitude for January-June 2020 in Figure 3. We can see that an anti-cyclonic type of airflow resides on the east oceans of China from February to April 2020. There is a westerly wind component in the northern branch of the anti-cyclonic airflow, especially in February and March of 2020. This westerly wind component becomes dominant and stronger at 850mb altitude and covers much broader east coastal regions (see Figure S1). Anthropogenic pollutants emitted and uplifted over the land are transported offshore to the downwind oceanic regions by this westerly airflow. Thus, the effect of emission reduction due to the lockdown over China may be brought to the downwind oceanic regions by the offshore transport, resulting in AOT reduction. In fact, Kanazawa University Wajima Air Monitoring Station (KUWAMS), located in western Japan and downwind of mainland China, is constantly under the influence of polluted air masses originating from China in the cold season. The concentration of particulate polycyclic aromatic hydrocarbons (PAHs) observed at KUWAMS decreased by 52.6%, 36.6%, and 36.7%, respectively, in February, March, and April 2020 compared with the same months in the previous year [27], which is consistent with our AOT reduction. Airflow changes to a very different monsoon flow pattern in May and June and associated AOT inter-annual variabilities probably become dominant. For example, a similar anti-cyclonic type of flow is also observed over the east oceans of China from January to March 2019 (see supplemental Figure S2). However, a change to monsoon flow pattern started earlier in 2019 (April) than in 2020 (May) but with a slower pace. AOT values over the downwind oceanic regions in April and May 2020 were higher rather than lower than the corresponding AOT values of 2019, which was due to the stronger offshore transport in springtime 2020 compared to springtime 2019, especially in April.

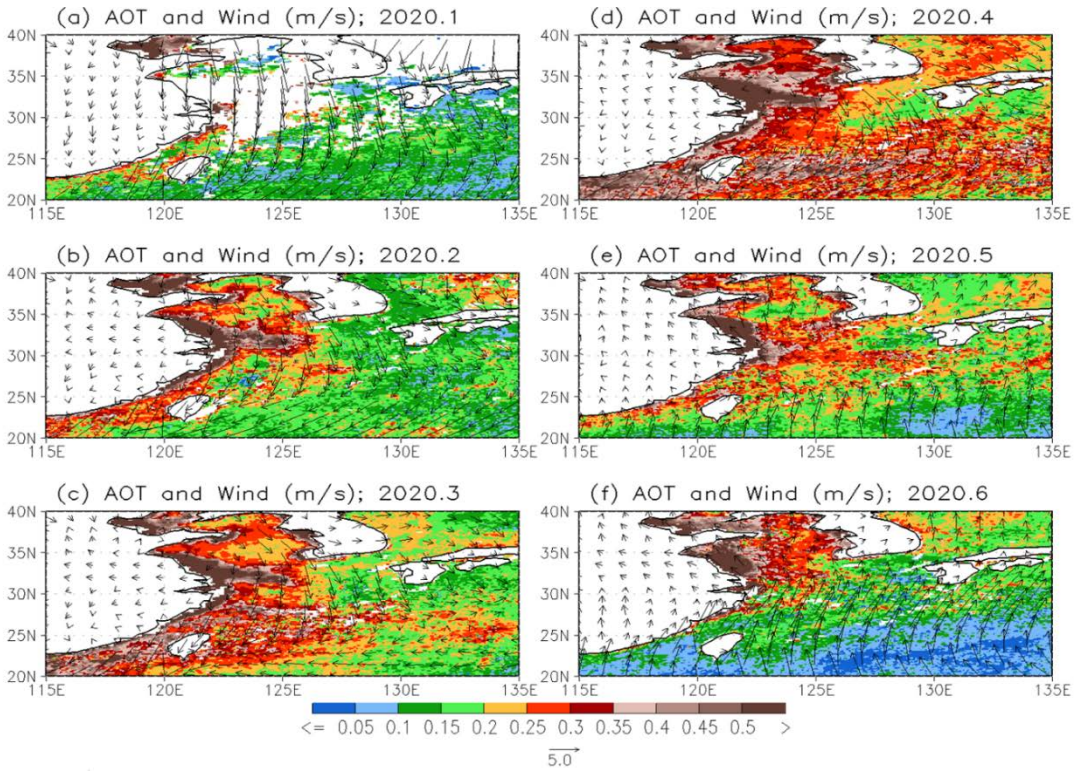

Figure 3 AOT distribution overlaid with wind speed (m/s) at 10m altitude for January-June 2020 in the downwind east oceanic regions of China.

The two types of relative monthly AOT differences in percentage for two coastal megacities, Shanghai and Tianjin, are summarized in Table 2 along with the result for the east coastal oceans of China defined in Table 1. The two types of monthly AOT differences over the water surface around the two coastal megacities and over the east coastal oceans of China show consistent negative values in the stringent lockdown months from January to March. The consistent negative values disappear in April, May, and June when the lockdowns are lifted gradually and AOT inter-annual variations in the Chinese monsoon season become dominant and obscure the AOT variation resulting from the relaxed confinement measures.

Table 2 Percentage changes of monthly AOT during the lockdown period of the COVID-19 pandemic relative to their corresponding monthly values in 2019 (first number) or climatology values (in parenthesis) over the east oceans of China and two megacities on the east coastal line.

Month	East Coastal Oceans of China	Shanghai	Tianjin
2020.1*	-21.41 (-31.32)	-37.53 (-39.34)	-8.40 (-3.17)
2020.2	-7.28 (-24.36)	-31.54 (-27.37)	-9.33 (-12.41)
2020.3^{+}	-9.20 (-22.31)	-7.26 (-25.42)	12.65 (-27.88)
2020.4	28.84 (-9.23)	27.06 (-13.94)	14.74 (-17.11)
2020.5	11.17 (-25.35)	31.38 (-19.12)	19.97 (-22.71)
2020.6	-3.65 (-27.80)	8.19 (-22.83)	16.39 (7.80)

Note: Superscripts * and $^{+}$ mark the month that stringent lockdown started and ended, respectively.

Europe was the second continent hit hard by the COVID-19. Two Mediterranean countries, Spain and Italy, were the most severely impacted in Europe and confinement measures were implemented to prevent the spread of the coronavirus. Limited lockdowns started at the beginning of March 2020; more restricted lockdowns became effective from the middle of March to the end of April, and the lockdowns were gradually lifted starting in May. For normal years before the COVID-19 pandemic, the anthropogenic pollutants (e.g., NO_2, O_3, $PM_{2.5}$, and PM_{10}) are generally higher over the northern and central parts than over the southern part of Italy [8]. Since the coronavirus infection cases were mainly concentrated in the northern and central parts of Italy [8], the lockdown measures were also more stringent in northern and central cities than in southern cities. Even though the air quality improvement appeared mainly in the urban areas of northern and central parts of Italy during the lockdown period, reduced NO_X along with increased O_3 and a minor reduction in particulate matter ($PM_{2.5}$ and PM_{10}) were also observed in the urban areas of southern Italy [7]. Unlike what was observed over the east coastal oceans of China in Figure 2 for the lockdown period, the two types of AOT monthly differences did not show consistent changes over the coastal waters of Mediterranean Sea (MS) for the lockdown period of southern Europe (not shown here). This result corroborates the findings of the in-situ measurements that the air quality impact due to the lockdown is mainly concentrated on the northern and central parts of Italy [8]. Thus, AOT inter-

annual variations and long-term trends over MS are probably dominant and can conceal the AOT variation induced from the lockdown, which were not as stringent as in China (especially in the southern part of Europe). For example, there is an evident decreasing trend of AOT over MS in the past four decades (see supplemental Figure S3), which results in negative anomaly as shown by the negative values in the parenthesis of Table 3. For the AOT difference between 2020 and 2019, inter-annual variations other than the long-term trend may play a more important role on the AOT change, which results in the inconsistency in the AOT changing tendency of Table 3.

Table 3 Similar to Table 2 but for the Mediterranean Sea and two megacities on the Mediterranean coastal line during the lockdown period of the COVID-19 pandemic.

Month	Mediterranean Sea	Barcelona	Rome
2020.3*	26.35 (-21.30)	32.58 (-14.01)	27.82 (-26.05)
2020.4^{+}	-4.85 (-28.76)	42.42 (-28.78)	4.20 (-28.86)
2020.5	40.36 (-34.48)	38.55 (-36.38)	18.83 (-10.21)
2020.6	-9.82 (-39.42)	7.31 (-39.45)	-23.39 (-45.16)

Similar to the Mediterranean Sea, the two types of monthly AOT differences over the east coastal ocean of the United States show inconsistent changes (not shown here) for the confinement period of COVID-19 from March to June. In fact, even for the inland urban areas of big cities, whether the coronavirus confinement makes air cleaner is still inconclusive [28]. However, the two types of monthly AOT differences show evident negative values consistently only over the water surface around New York City in April (see Table 4) when the most stringent confinement was implemented. Similar to the MS, there is an evident decreasing trend of AOT over the east coastal ocean of USA in the past four decades (see supplemental Figure S3), which results in negative anomaly listed in the parenthesis of Table 4. For the AOT difference between 2020 and 2019, the inter-annual variations of AOT other than the negative long-term trend may be the dominant source of the variation, which conceal the variation of AOT over the downwind east coastal ocean caused by the relatively lose confinement measures of COVID-19 in the USA.

Table 4 Similar to Table 2 but for the US east coastal ocean and two cities on the coastal line during the lockdown period of the COVID-19 pandemic.

Month	East Coastal Ocean of USA	New York City	Charleston
2020.3*	8.82 (-22.27)	3.05 (-38.51)	19.08 (-15.90)
2020.4	9.17 (-37.72)	-4.07 (-36.70)	10.01 (-36.35)
2020.5	4.44 (-33.57)	3.92 (-33.32)	9.33 (-34.23)
2020.6^{+}	-2.45 (-37.93)	-0.73 (-37.54)	10.73 (-22.44)

The Indian government ordered a nationwide lockdown in early March and lifted it gradually in early May, with a conditional relaxation after April 20 for the regions where the spread of coronavirus had been contained effectively. Unintentionally improved air quality in urban areas, especially in northern India, was observed during the lockdown period due to the reduction of anthropogenic emissions [5, 6]. A recent study by Sharma et al. (2020) [10] using surface observation found that even though most of the ambient pollutants were reduced in India during the lockdown period, $PM_{2.5}$ could still increase due to unfavourable meteorology. Figure 4 shows the two types of monthly AOT differences during the lockdown period over the Indian coastal oceans. Interestingly, monthly AOT was enhanced unexpectedly over the coastal water surface in March and April 2020 relative to both their climatology and to the same months in 2019. If we look at Figure 5, in springtime, wind blows mainly along the coastal line of the Arabian Sea except over the northern coastal ocean, where wind blows mainly from ocean to land. Airflow from ocean to land is the major characteristic over the coastal ocean of the Bay of Bengal. Similar wind field (not shown here) is also observed at 850mb altitude except the magnitude is larger than near the surface. Thus, meteorological condition is unfavourable for the AOT change related to the lockdown over the coastal oceans. Moreover, there is an evident increasing trend of AOT over the Indian coastal oceans in the past four decades (see supplemental Figure S3), which may also result in the positive AOT anomaly and enhancement noticed in Figure 4. Similar AOT enhancement was also noticed during the winter lockdown period in the suburban areas of northern China, where air quality is generally poor in winter due to heavy anthropogenic pollution. Observational analysis and model simulation performed over northern China by Le et al. (2020) [11] for the initial lockdown period indicated that proper meteorological conditions, non-linear heterogeneous chemical production, and secondary aerosol formation together contributed to the unexpected AOT surge. Similar mechanisms may be involved in the unexpected AOT enhancement over the Indian coastal oceans during the stringent lockdown period in the pre-monsoon season since both countries are plagued with heavy anthropogenic pollution and the Indian population is much denser in the coastal regions. In fact, both in-situ and satellite measurements did indicate enhanced SO_2 (the major precursor of secondary aerosols) in some urban/suburban areas of southern India during the lockdown period [5, 6], which indirectly supports our interpretation of the mechanism of AOT enhancement over the coastal oceans of India during the stringent lockdown period in the pre-monsoon season. Future modelling simulations are needed to confirm and separate the above causes of AOT enhancement during the pre-monsoon season of 2020.

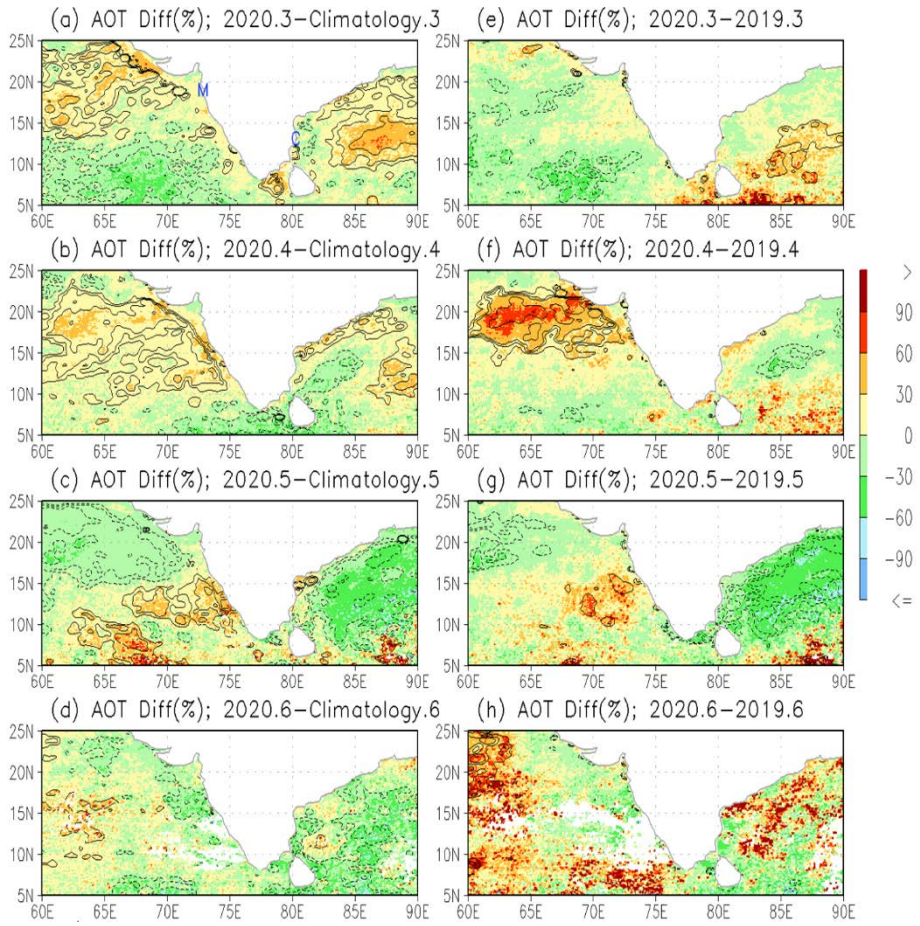

Figure 4 Similar to Figure 2 but for the Indian coastal oceans during the COVID-19 lockdown months. Blue capital letters M(umbai) and C(hennai) in panel (a) mark the positions of the two selected coastal cities.

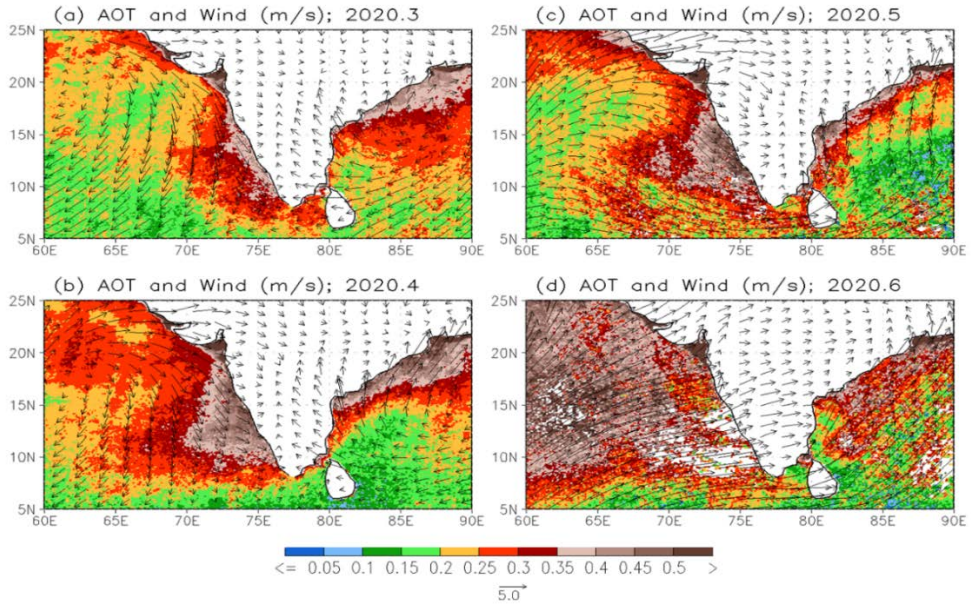

Figure 5 Similar to Figure 3 but for the Indian coastal oceans during the COVID-19 lockdown months.

In May, negative values appeared in both types of monthly AOT differences over the coastal ocean in the Bay of Bengal and propagated to the coastal ocean in the Arabian Sea in June. This is probably associated with the onset of the Indian monsoon in May and June, respectively, for the Bay of Bengal and the Arabian Sea [29-31], which may alter gas and heterogeneous chemistries along with aerosol formation and removal in the wet monsoon season. Actually, there are more missing AOT observations (see Figures 4d and 4h) in June due to persistent overcast skies in the Indian monsoon season. Thus, the AOT variation due to the inter-annual variability of the Indian monsoon in May and June 2020 is probably larger than the AOT variation induced from the lockdown that was already relaxed in May and June. In summary, the two-types of monthly AOT percentage differences for the Indian coastal oceans and two big cities, Mumbai and Chennai, on the coastal line are listed in Table 5.

Table 5 Similar to Table 2 but for the Indian coastal oceans and two big coastal cities during the lockdown period of the COVID-19 pandemic.

Month	Indian Coastal Oceans	Mumbai	Chennai
2020.3*	-0.77 (6.74)	1.80 (1.51)	5.72 (6.88)
2020.4	6.41 (7.68)	24.72 (11.63)	0.812 (-4.36)
2020.5+	-19.54 (-14.37)	5.45 (-5.72)	-35.77 (20.33)
2020.6	-4.91 (-12.75)	-13.80 (-13.48)	2.65 (-15.03)

4.2 AOT and Bushfires

The bushfires in Australia at the end of 2019 and the beginning of 2020 were the worst blaze in the past 25 years due to high temperatures and a prolonged drought in the region [14, 15] (https://www.statista.com/topics/6125/bushfires-in-australia/). The fires produced serious environmental and health consequence [17, 18]. Air quality was heavily damaged not only over the Australian continent but also over the entire southern ocean. Figure 6 shows AOT distribution overlaid with wind speed (m/s) at 10m altitude over the $10^oS - 50^oS$ latitude belt of the southern hemisphere (SH) for the four months of the 2019/2020 fire season in Australia. Strong westerly and easterly winds prevail over the latitude belt below and above 40^oS, respectively, for all four months. Westerly flow transported the smoke particles over the Australian continent from the burning areas in eastern Australia to the southern ocean in November and December 2019. In January 2020, higher AOT plumes transported eastward covered the whole latitude belt of westerly wind and even recycled back over Australia, causing an impact for a second time. Moreover, smoke plumes dispersed into the latitude belt of easterly wind above 40^oS also were blown to the whole latitude belt of easterly wind in January 2020. Smoke plumes diluted greatly in February 2020.

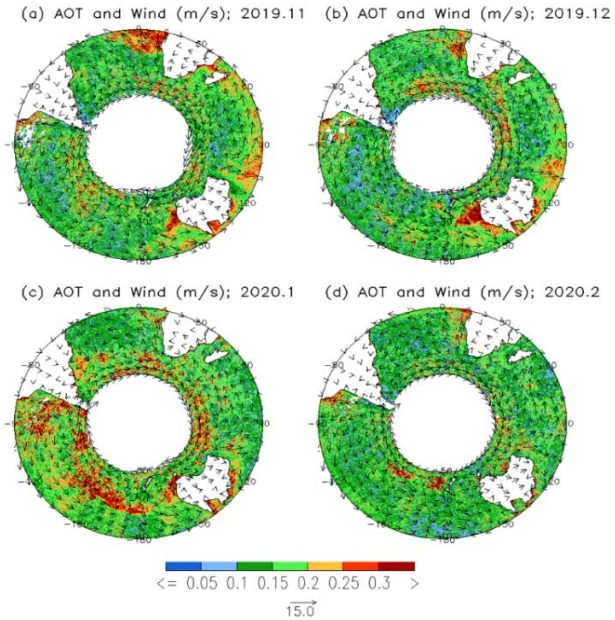

Figure 6 AOT distribution overlaid with wind speed (m/s) at 10m altitude over the 10°S − 50°S latitude belt of the southern hemisphere for the four months of the 2019/2020 fire season in Australia.

Figure 7 further displays the two types of relative monthly AOT differences (%) during the burning season over the 10°S − 50°S latitude belt of the southern hemisphere. AOT surge is most evident over the southeast coastal oceans of Australia due to heavy offshore smoke, which extends to the whole 10°S − 50°S latitude belt, and the enhancement is above 90%. AOT enhancement in magnitude and spatial spread reached a maximum in January 2020, the peak month of the fire season. Even though smoke plumes diluted greatly in February 2020 (see Figure 6d), the AOT enhancement is still significant and covers a broad area (see Figures 7d and 7h). The two types of monthly AOT differences in percentage over the water around two big coastal cities, Melbourne and Sydney, are provided in Table 6 along with the result for the east coastal ocean of Australia for the 2019/2020 fire season. AOT values are doubled in magnitude, which is much more significant than the AOT changes due to the lockdowns of the COVID-19 pandemic discussed above in subsection 4.1. Moreover, AOT values are monotonically augmented by the burning emissions over the Australian coastal oceans, while AOT changes due to the emissions reduction of the COVID-19 lockdowns discussed above are more irregular and relatively small over the downwind coastal oceans.

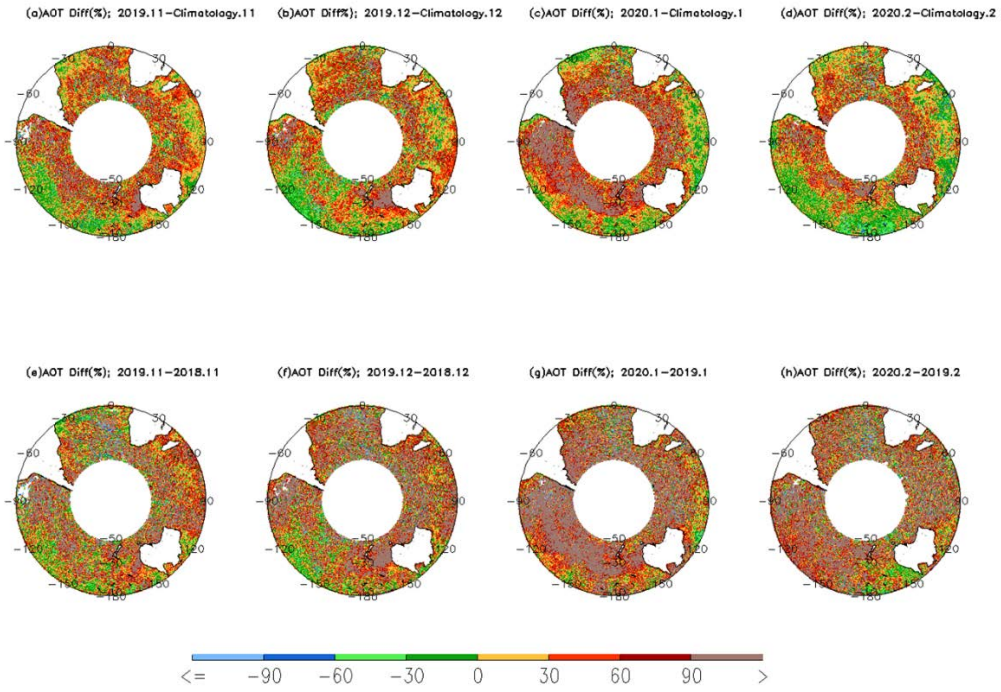

Figure 7 Distributions of relative monthly AOT anomaly (%) over the 10°S − 50°S latitude belt of the southern hemisphere (top panels) for the four months of the 2019/2020 fire season in Australia and the distributions of relative monthly AOT difference (%) for the same region (bottom panels) between the four months of the 2019/2020 and 2018/2019 fire seasons in Australia.

Table 6 The percentage augmentation of monthly AOT during the 2019/2020 fire season relative to the 2018/2019 fire season (first number) and their corresponding climatology values (in parenthesis) for the east coastal ocean of Australia and two big cities on the southeast coastal line.

Month	East Coastal Ocean of Australia	Melbourne	Sydney
2019.11	63.90 (61.14)	29.30 (19.99)	111.16 (114.08)
2019.12	97.93 (101.26)	61.05 (20.88)	228.95 (172.18)
2020.1	111.67 (105.54)	162.38 (133.28)	161.68 (184.28)
2020.2	15.75 (13.39)	36.91 (44.99)	50.05 (36.12)

5. Summary and Conclusions

Long-term AVHRR operational satellite AOT CDR is used to study the impact of COVID-19 lockdowns and Australian bushfires on aerosol loading over downwind oceanic regions influenced by offshore airflows. The coastal oceanic regions of five countries that were hit hard by the COVID-19 pandemic and the east coastal ocean of Australia, which was plagued by the 2019/2020 bushfires, are selected for our contrast study on the AOT response to the natural scenarios of emission

reduction due to the pandemic lockdowns and the enhancement due to the intensive bushfires. We found that AOT reduction is noticeable in the east coastal oceans of China during the stringent lockdown period of January, February, and March 2020 due to significant reduction of anthropogenic emissions. An unexpected surge of AOT also occurred in the pre-monsoon lockdown period over Indian coastal oceans, which is plagued regularly by offshore anthropogenic pollutions. This AOT surge may be due to complex and non-linear pollution chemistry and secondary aerosol formation under the favourable meteorological conditions of pre-monsoon season along with AOT inter-annual variations (including long-term trends) and needs to be confirmed in future studies with model simulations.

For the coastal oceanic regions with limited industrial pollution, and where confinement measures implemented for preventing the spread of the coronavirus in upwind countries were not strict, AOT changes due to the lockdown emission reduction may be concealed by the AOT inter-annual variation and long-term trends. In-depth studies based on model simulations are needed in the future for these observed vague impact scenarios. By contrast, AOT is significantly enhanced in a monotonic way due to the emissions from severe Australian bushfires, and the impact is not limited to the coastal oceans but affects the entire southern ocean, which may have important climate implications and deserves further study in the future through combined observations and model simulations. Because long-term AOT CDR based on heritage AVHRR satellite observation is available only over water surface, we can perform the analysis only on the selected mega-cities on the coastal line. In future work it would be worthwhile to study the other cities with less influence from the COVID-19 lockdown as a comparison by using other satellite observations and in-situ measurements. However, this impact study, which is based on long-term satellite observation in natural condition for two opposite emission scenarios associated with nature and human disasters, is still helpful in identifying effective mitigation strategies for future anthropogenic emissions and air pollution.

Acknowledgments

The author would like to acknowledge the invitation from guest editor Dr. Alfredo Moreira Caseiro Rocha to contribute this article to the special issue organized by him. The internal review by the Oceanographic and Geophysical Science and Services Division (OGSSD) at the National Centers for Environmental Information (NCEI) is also appreciated. Three reviewers' comments and suggestions helped improve the paper immensely. Proofreading of the paper by English editor Mark Essig of NCEI is greatly appreciated.

Additional Materials

The following additional materials are uploaded at the webpage of this paper.

1. Figure S1 : AOT distribution overlaid with wind speed (m/s) at 850mb altitude for January-June 2020 in the downwind east oceanic regions of China.
2. Figure S2: AOT distribution overlaid with wind speed (m/s) at 10m altitude for January-June 2019 in the downwind east oceanic region of China.

3. Figure S3: AOT long-term trend (1/decade) over the global ocean. The studied regions of China east oceans and the Indian coastal oceans are marked by the two blue rectangles, respectively.

Author Contributions

Xuepeng Zhao did all work.

Funding

The support from the base funding of the National Centers for Environmental Information (NCEI) at NOAA/NESDIS is acknowledged. The views, opinions, and findings contained in this paper are those of the author and should not be construed as an official National Oceanic and Atmospheric Administration or U.S. Government position, policy, or decision.

Competing Interests

The author has declared that no competing interests exist.

References

1. Sohrabi C, Alsafi Z, O'Neill N, Khan M, Kerwan A, Al-Jabir A, et al. World Health Organization declares global emergency: A review of the 2019 novel coronavirus (COVID-19). Int J Surg. 2020; 76: 71-76.
2. Chen K, Wang M, Huang C, Kinney PL, Anastas PT. Air pollution reduction and mortality benefit during the COVID-19 outbreak in China. Lancet Planetary Health. 2020; 4: e210-e212.
3. Chen QX, Huang CL, Yuan Y, Tan HP. Influence of COVID-19 event on air quality and their association in mainland China. Aerosol Air Qual Res. 2020; 20: 1541-1551.
4. Le Quéré C, Jackson RB, Jones MW, Smith AJ, Abernethy S, Andrew RM, et al. Temporary reduction in daily global CO_2 emissions during the COVID-19 forced confinement. Nat Clim Change. 2020; 10: 647-653.
5. Metya A, Dagupta P, Halder S, Chakraborty S, Tiwari YK. COVID-19 Lockdowns improve air quality in the South-east Asian regions, as seen by the remote sensing satellites. Aerosol Air Qual Res. 2020; 20: 1772-1782.
6. Navinya C, Patidar G, Phuleria HC. Examining effects of the COVID-19 national lockdown on ambient air quality across urban India. Aerosol Air Qual Res. 2020; 20: 1759-1771.
7. Sicard P, De Marco A, Agathokleous E, Feng ZZ, Xu XB, Paoletti E, et al. Amplified ozone pollution in cities during the COVID-19 lockdown. Sci Total Environ. 2020; 735: 139542.
8. Fattorini D, Regoli F. Role of the chronic air pollution levels in the Covid-19 outbreak risk in Italy. Environ Pollut. 2020; 264: 114732.
9. Kanniah KD, Kamarul Zaman NA, Kaskaoutis DG, Latif MT. COVID-19's impact on the atmospheric environment in the Southeast Asia region. Sci Total Environ. 2020; 736: 139658.
10. Sharma S, Zhang M, Gao J, Zhang H, Kota SH. Effect of restricted emissions during COVID-19 on air quality in India. Sci Total Environ. 2020; 728: 138878.
11. Le T, Wang Y, Liu L, Yang J, Yung YL, Li G, et al. Unexpected air pollution with marked emission reductions during the COVID-19 outbreak in China. Science. 2020; 369: 702-706.

12. Wang PF, Chen KY, Zhu SQ, Wang P, Zhang HL. Severe air pollution events not avoided by reduced anthropogenic activities during COVID-19 outbreak. Resour Conserv Recycl. 2020; 158: 104814.
13. Duncombe J. Five environmental consequences of Australia's fires [Internet]. Washington, DC: American Geophysical Union; 2020. Available from: https://eos.org/articles/five-environmental-consequences-of-australias-fires.
14. Boer MM, de Dios VR, Bradstock RA. Unprecedented burn area of Australian mega forest fires. Nat Clim Change. 2020; 10: 171-172.
15. Nolan RH, Boer MM, Collins L, de Dios VR, Clarke H, Jenkins MJ, et al. In the line of fire. Nat Clim Change. 2020; 10: 169.
16. Kablick III GP, Allen DR, Fromm MD, Nedoluha GE. Australian pyroCb smoke generates synoptic-scale stratospheric anticyclones. Geophys Res Lett. 2020; 4: e2020GL088101.
17. Filkov AI, Ngo T, Matthews S, Telfer S, Penman TD. Impact of Australia's catastrophic 2019/20 bushfire season on communities and environment. Retrospective analysis and current trends. J Safety Sci Resilience. 2020; 1: 44-56.
18. Borchers Arriagada N, Palmer AJ, Bowman DM, Morgan GG, Jalaludin BB, Johnston FH. Unprecedented smoke-related health burden associated with the 2019-20 bushfires in eastern Australia. Med J Aust. 2020; 6: 282-283.
19. Zhao TX, Laszlo I, Guo W, Heidinger A, Cao C, Jelenak A, et al. Study of long-term trend in aerosol optical thickness observed from operational AVHRR satellite instrument. J Geophys Res. 2008; 113: D07201.
20. Zhao XP, Heidinger AK, Walther A. Climatology analysis of aerosol effect on marine water cloud from long-term satellite climate data records. Remote Sensing. 2016; 8: 300.
21. Zhao XP, Dubovik O, Smirnov A, Holben BN, Sapper J, Pietras C, et al. Regional evaluation of an advanced very high resolution radiometer (AVHRR) two-channel aerosol retrieval algorithm. J Geophys Res. 2004; 109: D02204.
22. Zhao XP, Heidinger AK, Knapp KR. Long-term trends of zonally averaged aerosol optical thickness observed from operational satellite AVHRR instrument. Meteorol Appl. 2011; 18: 440-445.
23. Zhao XP, Liu YG, Yu FQ, Heidinger AK. Using long-term satellite observations to identify sensitive regimes and active regions of aerosol indirect effects for liquid clouds over global oceans. J Geophys Res. 2018; 123: 457-472.
24. Saha S, Moorthi S, Pan HL, Wu XR, Wang JD, Nadiga S, et al. The NCEP climate forecast system reanalysis. B Am Meteorol Soc. 2010; 91: 1015-1058.
25. Filonchyk M, Hurynovich V, Yan H, Gusev A, Shpilevskaya N. Impact assessment of COVID-19 on variations of SO_2, NO_2, CO and AOD over east China. Aerosol Air Qual Res. 2020; 20: 1530-1540.
26. Wan S, Cui K, Wang YF, Wu JL, Huang WS, Xu K, et al. Impact of the COVID-19 Event on trip intensity and air quality in southern China. Aerosol Air Qual Res. 2020; 20: 1727-1747.
27. Zhang L, Yang L, Zhou Q, Zhang X, Xing W, Zhang H, et al. Impact of the COVID-19 Outbreak on the long-range transport of particulate PAHs in East Asia. Aerosol Air Qual Res. 2020; 20: 2035-2046.
28. Schiermeier Q. Why pollution is plummeting in some cities-but not others [Internet]. London: Nature; 2020. Available from: https://www.nature.com/articles/d41586-020-01049-6.

29. Wu GX, Zhang YS. Tibetan Plateau forcing and the timing of the monsoon onset over South Asia and the South China Sea. Mon Weather Rev. 1998; 126: 913-927.
30. Zhang YS, Li T, Wang B, Wu G. Onset of the summer monsoon over the Indochina Peninsula: Climatology and interannual variations. J Climate. 2002; 15: 3206-3221.
31. Yamashima R, Matsumoto J, Takata K, Takahashi HG. Impact of historical land-use changes on the Indian summer monsoon onset. Int J Climatol. 2015; 35: 2419-2430.